

# An external potential dynamic study on the formation of interface in polydisperse polymer blends

Shuanhu Qi, Xinghua Zhang, and Dadong Yan\*

*Beijing National Laboratory for Molecular Sciences (BNLMS),*

*Joint Laboratory of Polymer Science and Materials,*

*Institute of Chemistry, Chinese Academy of Sciences, Beijing 100080, China*

(Dated: October 30, 2018)

## Abstract

The formation of interface from an initial sharp interface in polydisperse A/B blends is studied using the external potential dynamic method. The present model is a nonlocal coupling model as we take into account the correlation between segments in a single chain. The correlation is approximately expressed by Debye function and the diffusion dynamics are based on the Rouse chain model. The chain length distribution is described by the continuous Schulz distribution. Our numerical calculation indicates that the broadening of interface with respect to time obeys a power law at early times, and the power law indexes are the same for both monodisperse and polydisperse blend. The power law index is larger than that in the local coupling model. However there is not a unified scaling form of the broadening of the interface width if only the interfacial width at equilibrium is taken into account as the characteristic length of the system, because the correlation makes an extra characteristic length in the system, and the polydispersity is related to this length.

---

\*Electronic address: yandd@iccas.ac.cn

## I. INTRODUCTION

Polymers are often incompatible. When they are mixed together, an interface between them will occur. Because many properties of the blends are finally determined by the thickness of the interface and the concentration profile of the polymer across the interface, the equilibrium properties and dynamics of the interface attracted increased attention and gained widespread studies. The broadening of initially sharp interface between two types of polymers is of considerable interest.

Self-consistent field theory is a powerful method in the study of inhomogenous equilibrium systems [1, 2]. It can give detailed distribution of the monomer concentration across interface and specify other thermodynamic and structure quantities of interest. In order to study the kinetic pathway towards its equilibrium state. A method called “dynamic mean-field theory” (DMFT) [3, 4] or “dynamic density functional theory” (DDFT) [5, 6, 7] was developed. It is a generalized time-dependent Ginzburg-Landau theory for conserved order parameters. The volume fraction (concentration) is often chosen as the order parameter in polymer blends. In this theory, the free energy is calculated using the mean-field approximation, i.e., in each time step, the concentration and the potential should satisfy the self-consistent equations. This free energy is more exact than the Flory-Huggins type and the Ginzburg-Landau-Wilson type free energy which are both a local free energy plus the square gradient term of the concentration. In DMFT or DDFT, the Onsager kinetic coefficients are crucial quantities. Various chain dynamics and interactions will result different forms of kinetic coefficients. A simple one is the local coupling form which neglects the non-local interactions. In fact, sometimes the kinetic coefficients are assumed to be constants. If the dynamics of polymer chains are described by Rouse model, a different form of kinetic coefficient will be obtained, and the coupling between concentrations can be approximately described by Debye function in a homogenous homopolymer melt [7]. In the reptation regime, many researchers argued that the forms of the kinetic coefficient were the same as that for Rouse dynamics in a homogeneous polymer melt [8, 9, 10, 11], i.e., proportional to the Debye function. However, Maurits and Fraaije [7] found that the kinetic coefficients of the two different dynamics are not the same though do not differ very much. Wang and Shi [12] studied the interdiffusion process between incompatible polymers using the Flory-Huggins type free energy plus the square gradient term of the concentration. The growing of the interfacial width  $W$  obeys

the general scaling form  $W(t) \propto t^\alpha$ . It is found that the exponent  $\alpha$  is smaller than 0.25 for all the cases in their studies. As the square gradient approximation is only valid near the critical point, it is appropriate to obtain a more exact free energy which should also be valid far away from the critical point. The DMFT is the desirable method. Using DMFT with the local coupling approximation, Yeung and Shi [4] studied the dynamics of polymer interfaces. They found that the exponent  $\alpha$  is about 0.25 at early times, and is independent of the Flory-Huggins parameter  $\chi$  and the chain length. The interfacial width saturates to its equilibrium thickness at long times. Many experiments also focused on the interdiffusion process of a system with an initially sharp interface [13, 14, 15, 16, 17]. These experiments found that the broadening of the interface obeys a power law at early times, and it needs a very long time to saturate to its equilibrium thickness. It was also found that the exponent  $\alpha$  was in a range from 0.25 to 0.4, and decreases as the temperature is lowered [13]. One argued that the quick increase of the initial broadening is expected to be controlled by the fast single-chain mobility, while the long time saturation to the equilibrium thickness is due to the large-scale hydrodynamic flow [17].

The dynamics of polymer interfaces are often described by the time evolution of the concentration of the chains across the interfaces. In DMFT, this can be done by solving the time-dependent Ginzburg-Landau equation which the concentration satisfies. As this equation is usually solved numerically in real space, the Onsager coefficient is approximated as a local coupling form for the simplicity and saving time in calculation [3, 4, 5]. Since the concentration is a conserved quantity and it is linear related to the auxiliary potential field [18, 19], we expect that the auxiliary potential field is also conserved. The time-dependent Ginzburg-Landau equation with respect to concentration can be transformed to the form in which the auxiliary potential field is treated as the variable. Then we can obtain the external potential dynamic (EPD) model, as the equation is for the auxiliary potential fields. The EPD model is first proposed by Maurits and Fraaije. There are some advantages of the EPD method compared to DMFT method [20]. It incorporates a non-local coupling Onsager coefficient corresponding to the Rouse dynamics. In the spectral space, this can be realized through a local Onsager coefficient. Also, it is proved that numerically the EPD equation converges more easily and faster. In the present work we adopt the EPD method.

Polymer chains in the real system are always polydisperse, and polydispersity may play important roles in determining the properties of materials. Polydispersity enriches the phase

behavior at equilibrium [21] and decreases the free energy barrier of nucleation in meta-stable state of polymer blends [22]. The effort of polydispersity on the profile of the interface at equilibrium are studied by Fredrickson and Sides [23] in polydisperse polymer blends. In the present work, we studied the dynamics of interfaces in polydisperse blends.

This paper is organized as follows. In Sec. II we present the derivation of the EPD model based on the Rouse chain dynamics. The methods for solving the EPD equations are also talked. In Sec. III the main results and discussion are presented. In Sec. IV we summarize our conclusions.

## II. EXTERNAL POTENTIAL DYNAMIC MODEL

In the present work we consider an incompressible polymer blend of type A and type B linear, flexible homopolymers in which both species have polydisperse chain lengths. These two species of chains are modeled as Gaussian chains. To study the interfacial problems, it is convenient to work in the canonical ensemble. For simplicity the distributions of chain length for both species are described by the same prescribed function  $P(N)$ , where  $N$  is the degrees of polymerization, thus they have the same number- and weight-average chain lengths. Also both A and B monomers are assumed to have the same monomeric volume  $\rho_0^{-1}$  and Kuhn lengths  $b$ . In this section we first derived the time evolution equation the concentration satisfies based on the Rouse dynamics in the polydisperse A/B blend. Similar derivation in the monodisperse case can be found [7]. Then this equation of motion has been transformed to the EPD form. The EPD equations are then solved numerically.

### A. Rouse dynamics

Suppose that a polymer chain of type A with length  $N$  is subjected to an external force  $f_A[\mathbf{R}_N(s)]$ , where  $\mathbf{R}_N(s)$  denotes the position of monomer  $s$ . In the Rouse regime, as the correlations due to internal forces relax faster than the coarse-grained collective dynamics. Thus the chain can be considered as drifting with a constant velocity [7, 24]

$$v_d = \frac{D_0}{N} \int_0^N ds f_A[\mathbf{R}_N(s)], \quad (1)$$

where  $D_0$  is the diffusion coefficient of a monomer. It is important to found from Eq. (1) that the drift velocities of chains with different lengths are different, while the velocities are

the same for all beads in the same chain. The microscopic density of A species is defined as

$$\hat{\rho}_A(\mathbf{r}) \equiv \sum_{N=1}^{\infty} \sum_{i=1}^{n_{AN}} \int_0^N ds \delta[\mathbf{r} - \mathbf{R}_N^i(s)]. \quad (2)$$

Here,  $n_{AN}$  is the number of A chains for chain length  $N$ . The density can be alternatively expressed in the continuous limit by the following form,

$$\hat{\rho}_A(\mathbf{r}) = n_A \int_0^{\infty} dN P(N) \int_0^N \delta[\mathbf{r} - \mathbf{R}_N(s)], \quad (3)$$

where  $n_A$  is the total number of A chains. According to the equation of continuity and using the chain rule, we obtain,

$$\frac{\partial}{\partial t} \hat{\rho}_A(\mathbf{r}, t) = -n_A \int_0^{\infty} dN P(N) \int_0^N ds \nabla_{\mathbf{r}} \delta[\mathbf{r} - \mathbf{R}_N(s)] \cdot \frac{\partial \mathbf{R}_N(s)}{\partial t}. \quad (4)$$

We then replace  $\partial \mathbf{R}_N(s)/\partial t$  by Eq. (1), and the external force can be expressed by minus the gradient of the chemical potential. By some calculation we obtain,

$$\frac{\partial}{\partial t} \hat{\rho}_A(\mathbf{r}, t) = D_0 n_A \nabla_{\mathbf{r}} \cdot \int d\mathbf{r}' \int_0^{\infty} dN \frac{P(N)}{N} \int_0^N ds \int_0^N ds' \delta[\mathbf{r} - \mathbf{R}_N(s)] \delta[\mathbf{r}' - \mathbf{R}_N(s')] \nabla_{\mathbf{r}'} \mu_A(\mathbf{r}'), \quad (5)$$

where  $\mu_A$  is the chemical potential for A species. The concentration or the volume fraction of A species is defined by  $\phi_A(\mathbf{r}) = \langle \hat{\rho}_A \rangle / \rho_0$ , where  $\langle \dots \rangle$  denotes the ensemble average. Then we can obtain

$$\frac{\partial}{\partial t} \phi_A(\mathbf{r}, t) = D_n \bar{\phi}_A \nabla \cdot \int d\mathbf{r}' \int_0^{\infty} dN P(N) N g_D(\mathbf{r} - \mathbf{r}', N) \nabla_{\mathbf{r}'} \mu_A(\mathbf{r}'). \quad (6)$$

Here  $D_n = D_0/N_n$ ,  $N_n$  is the number-average chain length of A species,  $\bar{\phi}_A$  is the average volume fraction,  $\bar{\phi}_A = n_A N_n / \rho_0 V$ , where  $V$  is the volume of the system. The following relation has been used in deriving Eq. (6),  $\int_0^N ds \int_0^N ds' \delta[\mathbf{r} - \mathbf{R}_N(s)] \delta[\mathbf{r}' - \mathbf{R}_N(s')] = N^2 g_D(\mathbf{r} - \mathbf{r}', N)/V$ , where  $g_D(\mathbf{r} - \mathbf{r}', N)$  is the Debye function with chain length  $N$ , and it is valid for Gaussian chains [24]. Similarly we can obtain the time evolution equation for  $\phi_B(\mathbf{r}, t)$ . However,  $\phi_A(\mathbf{r}, t)$  and  $\phi_B(\mathbf{r}, t)$  are not independent, they should satisfy the incompressible condition,  $\phi_A(\mathbf{r}, t) + \phi_B(\mathbf{r}, t) = 1$ . The incompressible condition can be incorporated to the dynamic equation through introducing a potential  $U(\mathbf{r})$  which can be added to the chemical potential. After eliminating this potential from the time evolution equations for  $\phi_A(\mathbf{r}, t)$  and  $\phi_B(\mathbf{r}, t)$ , we can obtain,

$$\frac{\partial}{\partial t} \phi(\mathbf{r}, t) = \nabla \cdot \int d\mathbf{r}' \Lambda(\mathbf{r}, \mathbf{r}') \nabla_{\mathbf{r}'} \mu_{\phi}(\mathbf{r}'). \quad (7)$$

Here,  $\phi(\mathbf{r}) = \phi_A(\mathbf{r}) - \phi_B(\mathbf{r})$  is the concentration difference,  $\Lambda(\mathbf{r}, \mathbf{r}') = 2D_n \bar{\phi}_A \bar{\phi}_B \int_0^\infty dNP(N) Ng_D(\mathbf{r} - \mathbf{r}', N)$  is the Onsager kinetic coefficient.  $\bar{\phi}_B$  is the average volume fraction of B species,  $\bar{\phi}_B = n_B N_n / \rho_0 V$ , where  $n_B$  is the total number of B chains.  $\mu_\phi(\mathbf{r}) \equiv \mu_A(\mathbf{r}) - \mu_B(\mathbf{r})$  is the chemical potential difference. In the self-consistent theory, the chemical potentials are given by  $\delta F / \rho_0 \delta \phi_A$  and  $\delta F / \rho_0 \delta \phi_B$ .  $F$  is the free energy in the canonical ensemble:

$$F = \rho_0 \int d\mathbf{r} \chi \phi_A(\mathbf{r}) \phi_B(\mathbf{r}) - \rho_0 \sum_{\alpha=A,B} \int d\mathbf{r} \omega_\alpha(\mathbf{r}) \phi_\alpha(\mathbf{r}) - \sum_{\alpha=A,B} n_\alpha \int_0^\infty dNP(N) \ln Q_\alpha(\omega_\alpha, N). \quad (8)$$

Here,  $\omega_\alpha$  are the auxiliary fields conjugated to  $\phi_\alpha$ ,  $Q_\alpha[\omega_\alpha, N]$  are the single chain partition functions of the chain length  $N$  for  $\alpha$  species.

## B. External potential dynamic equation

We have mentioned that concentration is a conserved quantity and it is linear related to the auxiliary potential field, then the external potential field can be treated as a conserved variable. The dynamics of this potential can be described by the equation of the time-dependent Ginzburg-Landau form. The free energy of the system can also be written as a functional of the external potentials [2, 23, 25], which has the form of

$$H[\mu_+, \mu_-] = \int d\mathbf{r} \left( \frac{\rho_0}{\chi} \mu_-^2 - \rho_0 \mu_+ \right) - n_A \int_0^\infty dNP(N) \ln Q_A[\mu_+ - \mu_-, N] - n_B \int_0^\infty dNP(N) \ln Q_B[\mu_+ + \mu_-, N]. \quad (9)$$

Here,  $\mu_+ \equiv (\omega_A + \omega_B)/2$ ,  $\mu_- \equiv (\omega_B - \omega_A)/2$  are treated as the external potentials. The external field  $\mu_-$  couples the the concentration difference  $\phi_A - \phi_B$ , while  $\mu_+$  couples to the total concentration  $\phi_A + \phi_B$ . As there are two external fields in  $H$ , the numerical evaluation of the functional integral on the fields is difficult, often a saddle point approximation will be made when the fields  $\mu_+$  is integrated [19], which means  $\delta H[\mu_+, \mu_-] / \delta \mu_+ |_{\mu_+ = \mu_+^*} = 0$ . This is consistent with the incompressible condition, i.e.

$$\phi_A[\mu_+^* - \mu_-] + \phi_B[\mu_+^* + \mu_-] = 1. \quad (10)$$

The external potential dynamics can be expressed as

$$\frac{\partial}{\partial t} \mu_-(\mathbf{r}) = \nabla \cdot \int d\mathbf{r}' \Lambda_{\text{EPD}}(\mathbf{r}, \mathbf{r}') \nabla_{\mathbf{r}'} \frac{\delta H[\mu_+^*, \mu_-]}{\rho_0 \delta \mu_-}. \quad (11)$$

Here,  $\Lambda_{\text{EPD}}(\mathbf{r}, \mathbf{r}')$  is the Onsager coefficient in EPD model, and it is related to  $\Lambda(\mathbf{r}, \mathbf{r}')$ . The explicit expression of  $\Lambda(\mathbf{r}, \mathbf{r}')$  can be obtained from Eq. (7). According to the chain rule

$$\frac{\partial \phi(\mathbf{r}, t)}{\partial t} = \int d\mathbf{r}' \frac{\delta \phi(\mathbf{r}, t)}{\delta \mu_-(\mathbf{r}', t)} \frac{\partial \mu_-(\mathbf{r}', t)}{\partial t}, \quad (12)$$

where  $\partial \mu_+ / \partial t = 0$  has been used. According to the linear response theory, using the saddle point approximation, for Gaussian chains at any time we can obtain

$$\phi_A(\mathbf{r}) = -\frac{n_A}{\rho_0} \int_0^\infty dNP(N) \frac{\delta Q_A[\omega_A]}{\delta \omega_A(\mathbf{r})}, \quad (13)$$

and

$$\frac{\delta \phi_A(\mathbf{r})}{\delta \omega_A(\mathbf{r}')} = -\frac{n_A}{\rho_0} \int_0^\infty dNP(N) \frac{\delta^2 \ln Q_A}{\delta \omega_A(\mathbf{r}) \delta \omega_A(\mathbf{r}')} = -\frac{n_A}{\rho_0 V} \int_0^\infty dNP(N) N^2 g_D(\mathbf{r} - \mathbf{r}', N). \quad (14)$$

Similarly, we can obtain the expressions for  $\delta \phi_B(\mathbf{r}) / \delta \omega_B(\mathbf{r}')$ , and  $\delta \phi_A(\mathbf{r}) / \delta \omega_B(\mathbf{r}') = \delta \phi_B(\mathbf{r}) / \delta \omega_A(\mathbf{r}') = 0$ . For the incompressible Gaussian chain system, after some calculations, we can get

$$\frac{\delta \phi(\mathbf{r})}{\delta \mu_-(\mathbf{r}')} = -2 \frac{\delta[\phi_A(\mathbf{r}) - \phi_B(\mathbf{r})]}{\delta[\omega_A(\mathbf{r}') - \omega_B(\mathbf{r}')] } = 4\bar{\phi}_A \bar{\phi}_B \int_0^\infty dNP(N) \frac{N^2}{N_n} g_D(\mathbf{r} - \mathbf{r}', N). \quad (15)$$

Insert Eq. (15) into Eq. (12) and compare with Eq. (7), and also through a Fourier transformation, the EPD equation can be obtained in the spectral space

$$\frac{\partial \mu_-(\mathbf{q})}{\partial t} = \frac{D_n \chi}{2} \frac{\int_0^\infty dNP(N) N g_D(\mathbf{q}, N)}{\int_0^\infty dNP(N) \frac{N^2}{N_n} g_D(\mathbf{q}, N)} q^2 \left[ -\frac{2\mu_-(\mathbf{q})}{\chi} + \phi_A(\mathbf{q}) - \phi_B(\mathbf{q}) \right], \quad (16)$$

where  $\phi_A$  and  $\phi_B$  are functionals of  $\mu_+^*$  and  $\mu_-$ , and  $\mu_+^*$  is determined by the incompressible condition, i.e., Eq. (10). The Onsager coefficient in spectral space has the form of

$$\Lambda_{\text{EPD}}(\mathbf{q}) = \frac{D_n \chi}{2} \frac{\int_0^\infty dNP(N) N g_D(\mathbf{q}, N)}{\int_0^\infty dNP(N) \frac{N^2}{N_n} g_D(\mathbf{q}, N)}, \quad (17)$$

where  $g_D(\mathbf{q}, N) = 2(x + e^{-x} - 1)/x^2$ ,  $x = R_g^2 q^2$ , and  $R_g = Nb^2/6$  is the radius of gyration. In the monodisperse limit,  $P(N) = \delta(N - N_n)$ , then  $\Lambda_{\text{EPD}}(\mathbf{q}) = D_0 \chi / 2N_n$ , which is consistent with the result obtained by Müller and Schmid [19]. In the present work, we adopt the continuous Schulz distribution for reflecting realistic chain length distribution. However, it is not intrinsic to our topics. The Schulz distribution has the form of

$$P(N) = \frac{N^{k-1} (k+1)^k}{N_w^k \Gamma(k)} \exp[-(k+1)N/N_w], \quad (18)$$

where  $N_w$  is the weight-average chain length,  $k$  is a parameter related to the polydispersity index, a smaller  $k$  corresponds to a more polydisperse distribution, and the infinity of  $k$  corresponds to the monodisperse case.

### C. Numerical calculation

In the present work, we consider a one-dimensional system, and  $\bar{\phi}_A = \bar{\phi}_B = 1/2$ . The EPD equation (Eq. (16)) and Eq. (10) are closed and solved numerically. We adopt the numerical method developed by Cenicerros and Fredrickson [2, 25], which is a semi-implicit Seidel relaxation scheme. In the present work we studied the healing process of an initially sharp interface. The initially sharp interface was prepared by a tangent function, and for A species, it is

$$\phi_{AI}(x) = \frac{\phi_{Ap} + \phi_{Am}}{2} + \frac{\phi_{Ap} - \phi_{Am}}{2 \tanh \eta} \tanh \left[ \eta \cos \left( \frac{2\pi x}{l_x} \right) \right], \quad (19)$$

where  $\phi_{Ap}$  and  $\phi_{Am}$  are the concentrations at the boundaries in a phase-separated system at equilibrium,  $p$  denotes the A-rich boundary, while  $m$  denotes the A-poor boundary.  $l_x$  is the length of the system,  $x$  ranges from  $-l_x/2$  to  $l_x/2$ . The parameter  $\eta$  determines the sharpness of the interface, and a larger  $\eta$  corresponds to a sharper interface. In the present work, we choose  $\eta = 100$  which is large enough in our study. The initial concentration for B species is  $\phi_{BI}(x) = 1 - \phi_{AI}(x)$ . However, in order to proceed the evolution of the EPD equation, we need the initial external potentials  $\mu_{I-}(x)$  and  $\mu_{I+}(x)$  which target the initial concentrations. This is realized by numerically solving the following equations

$$\begin{aligned} \phi_A[\mu_{I+}(x) - \mu_{I-}(x)] - \phi_{AI}(x) &= 0, \\ \phi_B[\mu_{I+}(x) + \mu_{I-}(x)] - \phi_{BI}(x) &= 0. \end{aligned} \quad (20)$$

We also use the semi-implicit Seidel relaxation scheme.

In the calculation of the concentrations  $\phi_\alpha(\mathbf{r})$  ( $\alpha = A, B$ ), the infinite integrations are performed using a Gauss-Laguerre quadrature formula. The concentration (see Eq. (13)) can be expressed as

$$\phi_\alpha(x) = \frac{(k+1)\bar{\phi}_\alpha}{\Gamma(k+1)} \int_0^\infty dM e^{-M} \frac{M^{k-1}}{Q_\alpha[M/k+1, \omega_\alpha]} \int_0^{M/k+1} ds q_\alpha \left( x, \frac{M}{k+1} - s \right) q_\alpha(x, s), \quad (21)$$

where  $M = (k+1)N/N_w$ . The Gauss-Laguerre quadrature formula is

$$\int_0^\infty dM e^{-M} f(M) = \sum_{i=1}^{n_G} \lambda_i f(M_i), \quad (22)$$

where the abscissas ( $M_i$ ) and weights ( $\lambda_i$ ) can be found in a mathematical handbook. This formula converges very rapidly, and we find that 8 points are sufficiently accurate for all cases. In the present work, we adopt  $n_G = 8$ .

The relations between the partition functions of the single chain ( $Q_\alpha$ ) and the end-integrated propagators ( $q_\alpha$ ) are  $Q_\alpha[N, \omega_\alpha] = \int dx q_\alpha(x, N)/l_x$ , where  $q_\alpha$  satisfy the modified diffusion equations, which have the form of

$$\frac{\partial q_\alpha(x, s)}{\partial s} = \frac{b^2}{6} \frac{\partial^2 q_\alpha(x, s)}{\partial x^2} - \omega_\alpha(x) q_\alpha(x, s), \quad (23)$$

with the initial conditions  $q_\alpha(x, 0) = 1$ . The modified diffusion equations are solved numerically using the pseudo-spectral method [2, 23] with periodic boundary conditions (This results two A-B interfaces). This method is unconditionally stable in any number of space dimension and have higher accuracy [26] than the Crank-Nicholson semi-implicit schemes in our experience. For the convenience some quantities are scaled in the calculation

$$x \rightarrow x/R_{gw}, \quad s \rightarrow s/N_w, \quad t \rightarrow tD_n/R_{gw}^2, \quad (24)$$

where  $R_{gw} = N_w b^2/6$ . We also used  $\chi N_w$  instead of  $\chi$  to characterize the incompatibility. The length of the system were chosen as  $l_x = 40$ , and the number of spatial grid was  $N_x = 512$ , which means a mesh size of  $\Delta x = 0.078125$ . In solving the modified diffusion equations the prescribed contour steps were  $\Delta s \leq 0.0025$ , which ensured a eight-figure accuracy of the concentration profile. The time step was chosen smaller at early time and larger approaching equilibrium at later times. We also conformed that our results were independent of the mesh size and the system size by varying  $\Delta x$  and  $l_x$ .

### III. RESULTS AND DISCUSSION

In order to study the effect of polydispersity on the formation of interface, we first investigated the evolution of interface in the case of monodisperse A/B blend. The model we used in the monodisperse case was a simplified one of the present polydisperse model, which is also a nonlocal coupling one.

Figure 1 shows an example of the time evolution of the density profile in the monodisperse case, in which the volume fraction of A species  $\phi_A(x)$  at different times for  $\chi N=2.5$  is presented. The initial interface is very sharp, and it evolves to the equilibrium one eventually at long times. In this process, as show in Fig. 1 the  $\phi$ -enhanced and -depleted bumps appear, which were also observed in the local coupling model [4]. This can be understood by symmetry as explained by Yeung and Shi [4]. If we consider the interface at  $x = -10$ , and

the locations at  $x = -20$  and  $x = 0$  correspond to the phase boundaries at infinitely far away. The chemical potential is expressed as  $\mu = \delta F / \delta \phi$  ( $\phi$  means  $\phi_A$ ), and it equals to zero at  $x = -20$  and  $x = 0$ ; also the chemical potential is an odd function with respect to  $x = -10$ , hence  $\mu = 0$  at  $x = -10$ . There must be extremum values of the chemical potential between the interface and the phase boundaries, which is a maximum value on the A-rich side of the interface and a minimum value on the A-poor side. The diffusion of the order parameter satisfies  $j_x = -M(\phi)d\mu/d\phi$ , where  $j_x$  is the current and  $M(\phi) > 0$  is a dynamical coefficient. Near the interface,  $\phi$  is transported from the  $\phi$ -rich side of the interface to the  $\phi$ -poor side. However, the current changes its sign where the chemical potential is extremized. Therefore at some place far away from the interface,  $\phi$  must be transported away from the interface on  $\phi$ -rich side and towards the interface on  $\phi$ -poor side. This is why an enhancement of  $\phi$  above the equilibrium value on the A-rich side and a depletion on the A-poor side appear in the calculation. The calculation indicates that bumps are larger at smaller  $\chi N$ , while they are smaller at larger  $\chi N$ , and in the course of time the bumps move to the phase boundaries.

What we are interested in is the growth law of interfacial width with respect to time. The density across the interface is not homogeneous, thus the definition of the interfacial width is not unique. As a quantitative measure of the interfacial width, we followed Yeung and Shi, and also Steiner et al. [13] and chose the inverse of the maximum slope of  $\phi_A$  at the interface

$$W(t) = \left( \frac{1}{\Delta\phi_A} \frac{\partial\phi_A}{\partial x} \Big|_{x=-10} \right)^{-1}. \quad (25)$$

Here,  $\Delta\phi_A$  is the difference between the bulk value of  $\phi_A$  in the two equilibrium phases. It is obvious that this definition is sensitive to the local structure of the interface. Other definition, e.g. taking into account the entire structure of the interface, can alternatively be chosen, however, it dose not change the scaling relations.

Figure 2 shows the interfacial width defined in Eq. (25) as a function of time for different  $\chi N$ . The interfacial widths are divided by their equilibrium ones  $\xi$ . From the figure it can be seen that only at the very beginning the broadening of the interface obeys a power law with respect to time. In order to find this relation we rescale the time variable, which means a shift of the profile along  $t$ -axis. As shown in Fig. (3), if  $W(t)$  is sclaed by  $\xi$  and the time also scaled by  $\xi$ , all the data from Fig. 2 approximately collapse onto one single

master curve. It means that  $W(t)$  satisfies the following equation

$$W(t) = \xi f_{\text{mono}}(t/\xi^\beta), \quad (26)$$

where  $f_{\text{mono}}$  is a dimensionless function with  $f_{\text{mono}}(\infty) = 1$  and  $\beta = 1.0$ . It can be found from the figure that at the early times,  $W(t)$  satisfies the following equation  $W(t) \propto ct^\alpha$ , where  $c$ , a time independent constant, is related to  $\xi$ , and  $\alpha$  is the power law index. From the data fitting we found that  $\alpha$  approximately equals to 0.38. A direct scaling analysis using an expansion of the free energy to the second-order in  $\nabla\phi$  by the Cahn-Hilliard dynamics gives  $t^{-1} \propto W^{-4}$  or  $W \propto t^{1/4}$ . An more exact form of the free energy, the self-consistent mean field free energy with the Cahn-Hilliard dynamics also demonstrated  $W \propto t^{1/4}$ . It is easy to understand this relation since there is only one characteristic length  $\xi$  the equilibrium width of the interface in the approximated Cahn-Hilliard dynamic system. In the present model, we take into account the nonlocal coupling between segments of a single chain, hence, there exists another characteristic length, the correlation length. It is because of this correlation length, a simple scaling analysis with one characteristic length can not predict an exponent of 0.38. An prefactor of  $c$  is also a reflection of the existence of another characteristic length. This will be more precise in the polydisperse case, which will be talked later. An exponent of 0.38 lager than 0.25 means that the correlation between segments quicken the broadening of the interface.

In the following we consider the formation of interface in a polydisperse A/B blend. In the process of the evolution of the volume fraction of  $A$  species from its initially sharp distribution to the equilibrium diffusive distribution, the enhancement of  $\phi_A$  above the equilibrium value on the A-rich side of the interface and a depletion on the A-poor side are also observed in the numerical calculation. The magnitude of these bumps becomes smaller when  $\chi Nw$  becomes larger, and also the bumps move to the phase boundary as  $t$  grows. It is similar to the case that in monodisperse blend, and also can be understood by symmetry.

Figure 4 shows the evolution of interface with respect to time in the polydisperse polymer blends, the interfacial width is divided by  $\xi$ . The polydisperse parameters are chosen as  $k = 1, 2, \text{ and } 3$ , corresponding to the case that the polydispersity is reducing. The monodisperse case corresponds to an infinity of  $k$ . The incompatibility parameters are chosen as  $\chi Nw = 3.5, 4, 6, 8$  from weak segregation region to strong segregation region. From the figure it is seen that only at very early time there is a power law between the interfacial width and time.

In order to find this relation we also rescale the time variable. However, in the simulation we found that different forms of scaling of time were needed for different polydispersities. This is as expected since the extra characteristic lengths, the correlation lengths are different in blends with different polydispersities. There is not a unified scaling expression which contains only one characteristic length. Figure 5 shows the detailed information of forms of time scaling under which the data approximately collapse onto one single master curve for different polydispersities, respectively. From Fig. 5 (a) for the case of  $k = 1$  it can be found that if  $W/\xi$  is plotted as function of  $t/\xi^{1.9}$ , all data for different incompatibilities approximately collapse onto one single line; from Fig. 5 (b) and Fig. 5 (c), one can see that the scaling forms of time are  $t/\xi^{1.6}$  and  $t/\xi^{1.5}$  for  $k = 2$  and  $k = 3$ , respectively. It means that for a polydisperse polymer blend the broadening of interface satisfies

$$W(t) = \xi f_k(t/\xi^\beta), \quad (27)$$

where  $f_k$  is a dimensionless function with  $f_k(\infty) = 1$  and  $k$  denotes the polydispersity. From the simulation it is obvious that the parameter  $\beta$  decreases as the polydispersity decreases, and it approaches the value of monodisperse case 1.0 when  $k$  goes to infinity. Equation (27) demonstrates that there is not a unified scaling form of the broadening of the interface if we only take into account the equilibrium width of interface as the characteristic length. An unified scaling form which can include different case of polydispersities may be constructed if two characteristic lengths, the equilibrium width of interface and the correlation length, are taken into account. However, it is out of the present work. At the early time for all the polydisperse case the broadening of interface with respect to time satisfies  $W(t) \propto t^\alpha$ , where the power law  $\alpha \simeq 0.38$  which is the same as that in the monodisperse case. Thus we can conclude that the nonlocal coupling quickens the diffusion of polymer chains across the interface, while the polydispersity has no effect on the power law index.

#### IV. CONCLUSION

The formation of interface from an initially sharp one in polydisperse A/B blend is studied using external potential dynamic method. The chains of Both A and B species are polydisperse, and their chain length distributions are described by the continuous Schulz distribution. Based on the Rouse chain model, we derived the time evolution equation the

concentration satisfies. In the Rouse dynamics, the drift velocities of chains with different lengths are different, while the velocities are assumed to be the same for all beads in the same chain. The collective Rouse dynamics model is a nonlocal coupling model. This coupling is reflected by the Onsager coefficient which is related to the Debye function. The time evolution of the concentration then transformed to the EPD form, because of which are numerically more efficient to solve. The EPD equations are solved numerically using a semi-implicit Seidel relaxation scheme. Our calculation indicates that the broadening of interfacial width with respect to time obeys a power law at early times, and the power law indexes are the same for both monodisperse and polydisperse blend. This means that the polydispersity does not affect the form of this power law. The power law index is larger than that in the local coupling model. It is obvious that the nonlocal coupling quicken the diffusion of polymer chains across the interface. However there is not a unified scaling form of the broadening of the interfacial width if only the equilibrium interfacial width is taken into account as the characteristic length of the system, because there exists another characteristic length, the correlation length. The correlation lengths are different in blends with different polydispersities. An unified scaling form which can include different case of polydispersities may be constructed if two characteristic lengths, the equilibrium width of interface and the correlation length, are taken into account. This will be studied in the future.

## ACKNOWLEDGMENTS

We thank Prof. An-Chang Shi for the helpful discussion and suggestions. This work is supported by National Natural Science Foundation of China (NSFC) 20574085 and the Grant from Chinese Academy of Sciences KJCX2-YW-206.

- 
- [1] I. C. Sanchez, *Physics of Polymer Surfaces and Interfaces* (Butterworth-Heinemann: Boston MA, 1992).
- [2] G. H. Fredrickson, *The Equilibrium Theory of Inhomogeneous Polymers* (Clarendon Press, Oxford, New York, 2006).
- [3] R. Hasegawa and M. Doi, *Macromolecules* **30**, 3086 (1997)
- [4] C. Yeung and A.-C. Shi, *Macromolecules* **32**, 3637 (1999).
- [5] J. G. E. M. Fraaije, *J. Chem. Phys.* **99**, 9202 (1993).
- [6] J. G. E. M. Fraaije, B. A. C. van Vlimmeren, N. M. Maurits, M. Postma, O. A. Evers, C. Hoffmann, P. Altevogt, and G. Goldbeck-Wood, *J. Chem. Phys.* **106**, 4260 (1997).
- [7] M. Maurits and J. G. E. M. Fraaije, *J. Chem. Phys.* **107**, 5879 (1997).
- [8] P. Pincus, *J. Chem. Phys.* **75**, 1996 (1981).
- [9] K. Binder, *J. Chem. Phys.* **79**, 6387 (1983).
- [10] K. Kawasaki and K. Sekimoto, *Physica* **148A**, 361 (1988).
- [11] K. Kawasaki and K. Sekimoto, *Macromolecules* **22**, 3063 (1989).
- [12] S.-Q. Wang and Q. Shi, *Macromolecules* **26**, 1091 (1993).
- [13] U. Steiner, G. Krausch, G. Schatz, and J. Klein, *Phys. Rev. Lett.* **64**, 1119 (1990).
- [14] J. Klein, *Science* **250**, 640 (1990).
- [15] A. Losch, D. Woerman, and J. Klein, *Macromolecules* **27**, 5713 (1994).
- [16] M. Sferrazza, C. Xiao, R. A. L. Jones, and J. Penfold, *Philos. Mag. Lett.* **80**, 561 (2000).
- [17] W. Béziel, G. Fragneto, F. Cousin, and M. Sferrazza, *Phys. Rev. E* **78**, 022801 (2008).
- [18] F. Schmid, *J. Phys.: Condens. Matter* **10**, 8105 (1998).
- [19] M. Müller and F. Schmid, *Adv. Polym. Sci.* **185**, 1 (2005).
- [20] E. Reister, M. Müller, and K. Binder, *Phys. Rev. E* **64**, 041804 (2001)
- [21] P. Sollich, *J. Phys.: Condens. Matter* **14**, R79 (2002)
- [22] S. Qi and D. Yan, *J. Chem. Phys.* **129**, 204902 (2008).
- [23] G. H. Fredrickson and S. W. Sides, *Macromolecules* **36**, 5415 (2003).
- [24] M. Doi, *Introduction to Polymer Physics* (Clarendon, Oxford, 1996).
- [25] H. D. Ceniceros and G. H. Fredrickson, *Mult. Mod. Simulat.* **2**, 452 (2004)
- [26] Q. Wang, P. F. Nealey, and J. J. de Pablo, *Macromolecules* **35**, 9563 (2002)

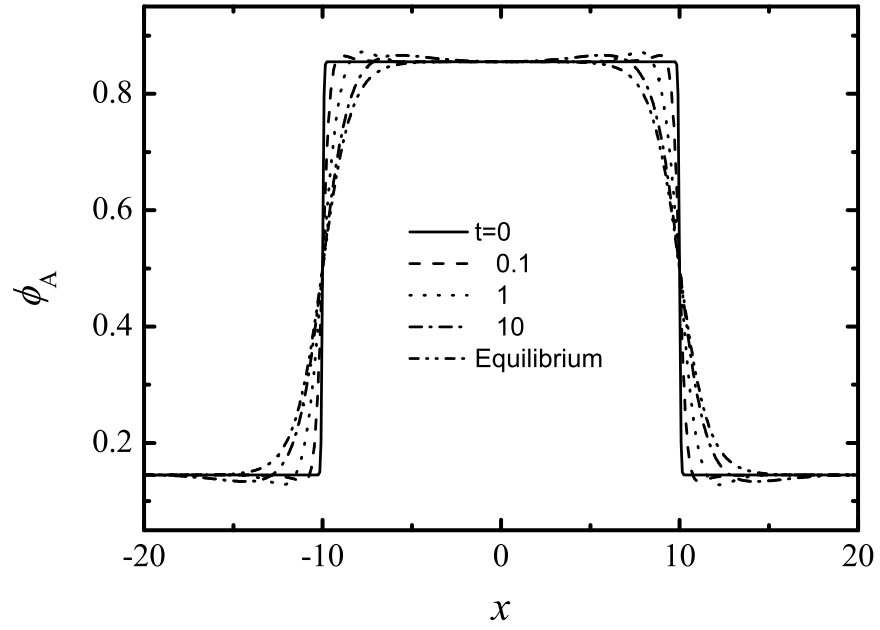


FIG. 1: Time evolution of the density profile in the monodisperse case for  $\chi N = 2.5$ . The  $\phi_A$ -enhanced and -depleted bumps appear, which can be explained by symmetry.

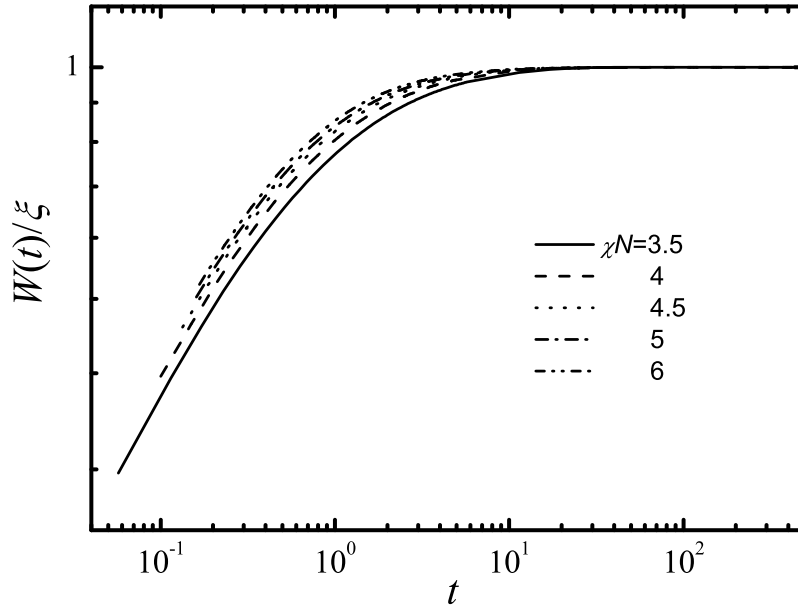


FIG. 2: The broadening of interface with respect to time for different  $\chi N$  in the monodisperse case. The interfacial width is scaled by  $\xi$ . It shows that at early times the interfacial widths broaden fast, and they saturate to the equilibrium ones at very long times.

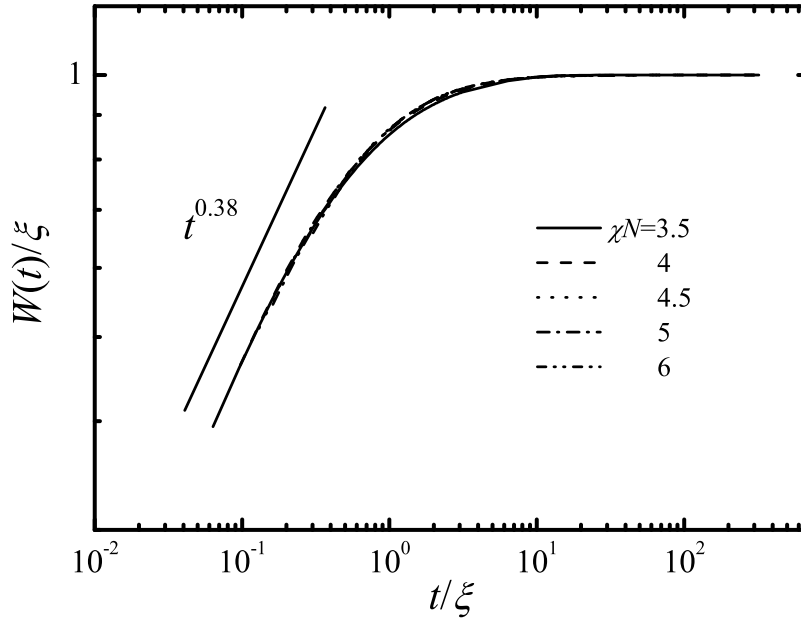


FIG. 3: Data from Fig. 2 plotted in a scaled form. Here the interfacial width is scaled by  $\xi$ , the time is also scaled by  $\xi$ . The data approximately collapse onto a single master curve. At early times, the broadening of interfacial width obeys a power law, and the power law index is about 0.38.

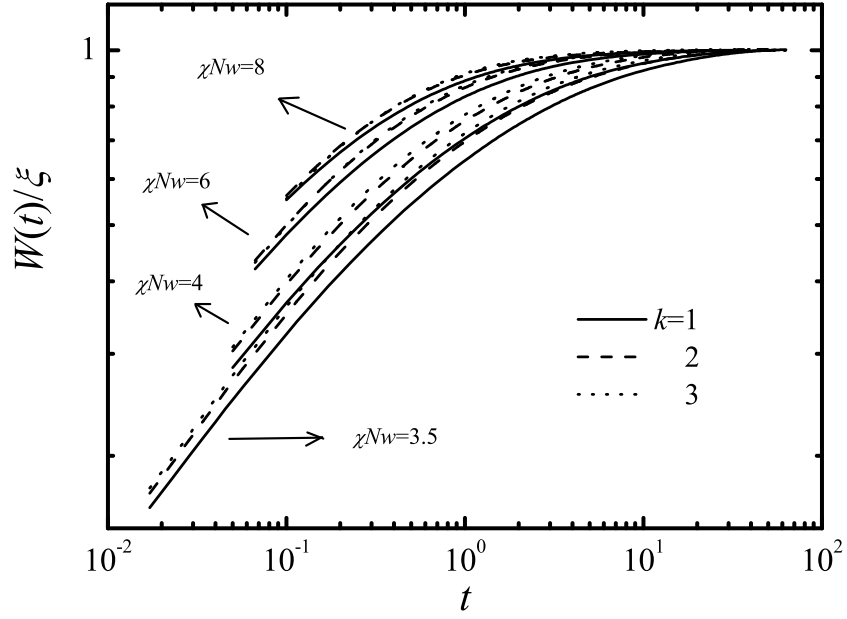


FIG. 4: The evolution of interface with respect to time in the polydisperse case for different  $\chi N_w$  and different polydispersities. The interfacial width is scaled by  $\xi$

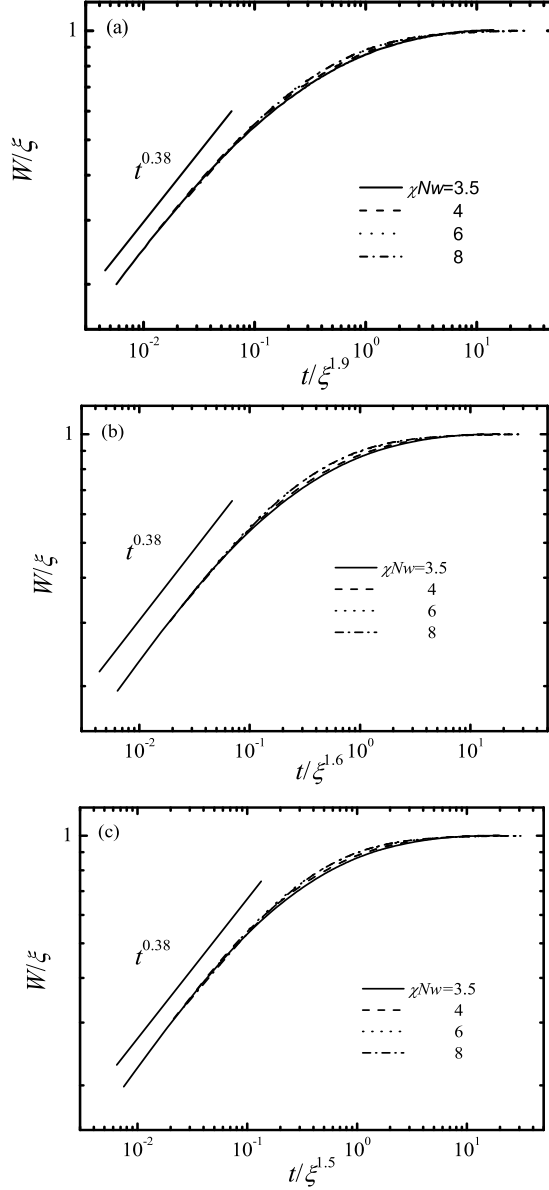


FIG. 5: Data from Fig. 3 plotted in a scaled form. Here the interfacial width is scaled by  $\xi$ , the time is also scaled by  $\xi^{1.9}$  for  $k = 1$  (a), by  $\xi^{1.6}$  for  $k = 2$  (b), and by  $\xi^{1.5}$  for  $k = 3$  (c). The exponent of  $\xi$  approaches the value that in the monodisperse case as  $k$  goes to infinity. The data approximately collapse onto a single master curve for different polydisperse case, respectively. At early times, the broadening of interfacial width obeys a power law, and the power law index is about 0.38 which is independent of the polydispersity.